

# A coupled hygro-chemo-mechanical damage model for ASR-affected concrete

Falko Bangert & Günther Meschke

*Institute for Structural Mechanics, Ruhr University Bochum, Germany*

**ABSTRACT:** The paper presents a hygro-chemo-mechanical model for ASR affected concrete, which is based on concepts of the Theory of Porous Media. Concrete is regarded as a mixture of three main interacting constituents: the skeleton, the pore liquid and the pore gas. The skeleton in turn represents a binary mixture of the unreacted, unswollen and the already reacted, swollen material. When ASR takes place, mass of the unreacted material is non-instantaneously converted into mass of the reacted material. Since the unreacted material is characterized by a smaller density, the material swells. The applicability of the model is demonstrated by a numerical simulation of the long-term degradation of an ASR-affected concrete beam subjected to a time-variant hygral loading history.

**Keywords:** deterioration, alkali-silica reaction, Finite Element Method, durability, structural analysis

## 1 INTRODUCTION

The durability of concrete structures is strongly influenced by the accumulation of damage caused by external loading in conjunction with structural degradation resulting from chemically induced deteriorating effects. The present paper is concerned with the macroscopic modeling and numerical simulation of the alkali-silica reaction (ASR) as a typical chemical expansive reaction in concrete.

On the micro-level the ASR deterioration can be attributed to a chemical reaction between the high alkaline pore liquid and reactive forms of silica within the aggregate particles (Glasser 1992). The reaction leads to the alkali-silica gel as reaction product. In the presence of water the gel swells, creating an increasing internal pressure. The swelling pressure causes excessive expansion, the development and propagation of cracks and a considerable reduction of the mechanical properties. Since the impact of the alkali-silica reaction is influenced by many factors (e.g. humidity, temperature), it is nearly impossible to make realistic predictions on a structural level solely based on the qualitative knowledge of the ASR chemistry. For the quanti-

tative assessment of the ASR deterioration in time and space a coupled hygro-chemo-mechanical damage model for ASR-affected concrete is developed within the framework of the Theory of Porous Media (Ehlers 2002). At the same level of observation, models for ASR-expansion of concrete have been proposed recently by Ulm et al. (2000) and Steffens et al. (2003).

## 2 MODEL FOR ASR-AFFECTED CONCRETE

### 2.1 *Experimental findings concerning ASR*

The alkali-silica reaction is characterized by two main mechanisms. Firstly, silica is dissolved from the aggregates, whereby a gel is formed and secondly, the swelling of the gel by imbibition of water, which results in the expansion and deterioration of the affected concrete.

Strictly speaking, any aggregate containing silica has the potential to participate in the alkali-silica reaction. Nevertheless, only the poorly crystalline, amorphous forms of silica are dissolved fast enough to form a swelling gel within the normal engineering time-scale (Glasser 1992). In a first step of the dissolution process, hydroxyl ions from the high al-

kaline pore solution attack the siloxane groups of the silicious constituents forming less stable silanol groups. In a second step, these silanol groups react with further hydroxyl ions. As more siloxane bonds are attacked by the dissolution process, a gel-like layer forms at the surface of the aggregates. Depending on the pH value of the pore liquid some silica may even pass into solution as monomeric species (Dent Glasser and Kataoka 1981).

Dron and Brivot (1993) reproduced the dissolution mechanism of silica in experimental studies using various kinds of silica, which were stored in solutions of sodium hydroxide. Their results show, that the dissolution of silica can be interpreted as a chemical reaction, which follows a first-order kinetic law (Atkins 1998). This means that the dissolution rate decreases linearly from an initial value, where the reaction starts, to zero, at which the silica is completely dissolved.

The gel which is formed by the aforementioned dissolution process is hydrophilic (Glasser 1992). This means, that the gel imbibes water, which results in the swelling of the gel. Although the gel is formed even at relatively low humidities, high moisture levels are required in order for the gel to imbibe water and increase in volume. In a sufficiently humid environment, the gel may expand into pores and cracks in the cementitious skeleton. Once this space providing free expansion of the gel is filled, the swelling is restrained and the gel exerts a pressure on the concrete skeleton. The swelling pressure induces expansions in localized regions which, in turn, lead to the opening and propagation of cracks and to the disruption of the affected concrete. This results in a drastic reduction of the mechanical properties and consequently to the degradation of ASR-affected concrete structures.

By comparing the time scales of the swelling of synthetic gels (Struble and Diamond 1981) and of concrete specimens (Larive 1998), it can be concluded, that the imbibition of water by a gel is much faster than the progress of deterioration in ASR-affected concrete. This leads to the conclusion, that the overall reaction rate of ASR is not governed by the imbibition of water by the gel but by the formation of the gel by the dissolution of silica.

## 2.2 Phenomenological description of ASR

According to the experimental findings discussed in the previous section, the alkali-silica reaction is regarded as a multistage process, which starts with

the non-instantaneous formation of a gel by the dissolution of silica. The progress of gel formation is described phenomenologically by the non-dimensional reaction extent  $\xi \in [0, 1]$ , where  $\xi = 0$  represents the beginning and  $\xi = 1$  the end of the dissolution process. The evolution of  $\xi$  in time is defined by a kinetic law. Adopting a first-order kinetic law reads as follows:

$$\frac{\partial \xi}{\partial t} = k [1 - \xi]. \quad (1)$$

Herein, the parameter  $k$  denotes the characteristic velocity. It has been found, that  $k$  strongly depends on the moisture content. More water accelerates the reaction significantly. This corresponds to an increasing characteristic velocity  $k$ . Integration of equation (1) for constant environmental conditions ( $k = \text{const.}$ ) yields the reaction extent  $\xi$  as a function of time  $t$ :

$$\xi = 1 - e^{-kt} \quad (2)$$

The non-instantaneous gel formation process is followed by the nearly instantaneous swelling of the gel, which results in the expansion and deterioration of the ASR-affected concrete. Since in a multistage process the slowest process controls the overall kinetics, it is reasonable to assume, that the alkali-silica reaction (formation of gel + swelling of gel) is governed by the kinetic law of the gel formation, which is represented by equation (1).

## 2.3 ASR-affected concrete as porous medium

Concrete is modeled as a partially saturated porous material, which is interpreted as a mixture  $\varphi$  of three main interacting constituents  $\varphi^\alpha$ , namely the skeleton (index  $\alpha = s$ ), the pore liquid (index  $\alpha = l$ ) and the pore gas (index  $\alpha = g$ ). The concrete skeleton itself represents a mixture of the aggregates, the gel and the cement paste. However, in the proposed model the skeleton is regarded as a binary mixture

$$\varphi^s = \varphi^u + \varphi^r \quad (3)$$

of an unreacted phase  $\varphi^u$  and a reacted phase  $\varphi^r$  without making any distinction between aggregates, gel and cement paste. The unreacted phase  $\varphi^u$  represents the unreacted, unswollen skeleton material *before* being affected by the alkali-silica reaction. On the other hand the reacted phase  $\varphi^r$  represents the reacted, swollen skeleton material *after completion* of ASR. During the alkali-silica reaction, mass

of the unreacted phase is non-instantaneously converted into mass of the reacted phase representing the gel formation process.

Following the standard concepts of the Theory of Porous Media, it is assumed, that the constituents  $\varphi^\alpha$  are homogenized over a representative volume element, which is occupied by the mixture  $\varphi = \varphi^s + \varphi^l + \varphi^g$ . Therefore, material points of each constituent  $\varphi^\alpha$  exist at each geometrical point  $\mathbf{x}$ . Hence, the local composition of the mixture  $\varphi$  is described by the volume fraction  $\phi^\alpha$ , which is defined as the ratio of the volume element  $dv^\alpha$  occupied by the individual constituent  $\varphi^\alpha$  and the volume element  $dv$  occupied by the mixture  $\varphi$ :

$$\phi^\alpha = \frac{dv^\alpha}{dv}. \quad (4)$$

Since the solid skeleton is regarded as a binary mixture, the respective volume fraction  $\phi^s$  is given as the sum of the volume fraction of the unreacted volume fraction  $\phi^u$  and the reacted volume fraction  $\phi^r$ :

$$\phi^s = \phi^u + \phi^r. \quad (5)$$

The material density  $\varrho^\alpha$  and the partial density  $\rho^\alpha$  of the constituent  $\varphi^\alpha$  are introduced as

$$\varrho^\alpha = \frac{dm^\alpha}{dv^\alpha}, \quad \rho^\alpha = \frac{dm^\alpha}{dv} = \phi^\alpha \varrho^\alpha. \quad (6)$$

Herein,  $dm^\alpha$  denotes the local mass of the volume element  $dv^\alpha$ . The partial density of the skeleton is assumed to be composed by an unreacted and a reacted part:

$$\rho^s = \phi^s \varrho^s = \phi^u \varrho^u + \phi^r \varrho^r. \quad (7)$$

Since the material densities of the unreacted and the reacted material are different ( $\varrho^u > \varrho^r$ ), a variation of the volume fractions  $\phi^u$  and  $\phi^r$  due to the aforementioned mass exchange results in a variation of the material density of the skeleton  $\varrho^s$ . Thus, the ASR-induced swelling of the skeleton is associated with the variation of the material density  $\varrho^s$ .

#### 2.4 Balance equations

Investigations on the role of water in the alkali-silica reaction have shown, that ASR has no appreciable influence on the moisture transport (Larive 1998). Thus, it is reasonable to neglect any mass exchange between the skeleton and the pore fluids. In doing so, the mass balance equation of the skeleton  $\varphi^s$  as a binary mixture reads (Ehlers 2002)

$$\frac{\partial[\phi^s \varrho^s]}{\partial t} + \text{div}(\phi^s \varrho^s \mathbf{x}'_s) = 0, \quad (8)$$

whereby  $\mathbf{x}'_s$  denotes the velocity of the skeleton.

It is assumed that the constituents  $\varphi^u$  and  $\varphi^r$  of the skeleton  $\varphi^s$  follow the same motion function and, therefore, exhibit the same velocity  $\mathbf{x}'_s = \mathbf{x}'_u = \mathbf{x}'_r$ . Providing that  $\varphi^u$  and  $\varphi^r$  are incompressible ( $\varrho^u, \varrho^r \rightarrow \text{const.}$ ), the associated partial mass balance equations result in the following volume balance equations:

$$\begin{aligned} \frac{\partial \phi^u}{\partial t} + \text{div}(\phi^u \mathbf{x}'_s) &= \frac{\partial \phi^{u \rightarrow r}}{\partial t}, \\ \frac{\partial \phi^r}{\partial t} + \text{div}(\phi^r \mathbf{x}'_s) &= \frac{\partial \phi^{r \leftarrow u}}{\partial t}. \end{aligned} \quad (9)$$

The terms on the right hand side represent the mass exchange between the phases  $\varphi^u$  and  $\varphi^r$  due to the dissolution process. Since the summation of the partial balances (9) must result in the mixture balance equation (8), the following constraint must hold:

$$\varrho^u \frac{\partial \phi^{u \rightarrow r}}{\partial t} + \varrho^r \frac{\partial \phi^{r \leftarrow u}}{\partial t} = 0. \quad (10)$$

Using the assumption, that the kinetics of the dissolution of silica and consequently the mass exchange between the constituents  $\varphi^u$  and  $\varphi^r$  follow a first order kinetic law, one may write (Atkins 1998)

$$\frac{\partial \phi^{u \rightarrow r}}{\partial t} = -k \phi^u, \quad \frac{\partial \phi^{r \leftarrow u}}{\partial t} = \frac{\varrho^u}{\varrho^r} k \phi^u, \quad (11)$$

whereby the parameter  $k$  is the aforementioned characteristic velocity. Inserting the equations (11) into the volume balance equations (9) and neglecting the skeleton velocity

$$\mathbf{x}'_s \approx 0 \quad (12)$$

yields:

$$\frac{\partial \phi^u}{\partial t} = -k \phi^u, \quad \frac{\partial \phi^r}{\partial t} = \frac{\varrho^u}{\varrho^r} k \phi^u. \quad (13)$$

For constant environmental conditions the volume balance equations (13) can be integrated analytically. With the initial value  $\phi_0^u$  one obtains

$$\phi^u = \phi_0^u [1 - \xi], \quad \phi^r = \frac{\varrho^u}{\varrho^r} \phi_0^u \xi, \quad (14)$$

where the overall reaction extent  $\xi$  according to equation (2) has been used. Finally, inserting (14) into (7) yields the material density of the skeleton  $\varrho^s$  as a function of the reaction extent  $\xi$ :

$$\varrho^s = \frac{\varrho^u \varrho^r}{\varrho^r + \xi [\varrho^u - \varrho^r]}. \quad (15)$$

Thus, expression (15) reflects the swelling state of the skeleton ranging from an unswollen state ( $\xi = 0 \rightarrow \varrho^s = \varrho^u$ ), if the alkali-silica reaction has not yet started, to a fully swollen state ( $\xi = 1 \rightarrow \varrho^s = \varrho^r$ ) after the ASR process has come to an end.

The mass balance equations of the pore fluids  $\varphi^\beta$  ( $\beta = l \rightarrow$  liquid phase,  $\beta = g \rightarrow$  gas phase) are given by:

$$\frac{\partial[\phi^\beta \varrho^\beta]}{\partial t} + \text{div}(\phi^\beta \varrho^\beta \mathbf{x}'_\beta) = 0. \quad (16)$$

Neglecting the compressibility of the pore liquid in comparison to the compressibility of the pore gas ( $\varrho^l \rightarrow \text{const.}$ ) and using the seepage velocities  $\mathbf{w}_\beta = \mathbf{x}'_\beta - \mathbf{x}'_s$  together with the assumption (12) one obtains from equation (16):

$$\begin{aligned} \frac{\partial \phi^l}{\partial t} + \text{div}(\phi^l \mathbf{w}_l) &= 0, \\ \frac{\partial[\phi^g \varrho^g]}{\partial t} + \text{div}(\phi^g \varrho^g \mathbf{w}_g) &= 0. \end{aligned} \quad (17)$$

## 2.5 Constitutive equations

In a partially saturated porous medium, a fundamental correlation between the liquid saturation  $s^l$

$$s^l = \frac{\phi^l}{\phi^l + \phi^g} \quad (18)$$

and the macroscopic capillary pressure  $p^c$

$$p^c = p^g - p^l \quad (19)$$

exists, whereby  $p^\beta$  is the effective pressure of the pore fluid  $\varphi^\beta$ . Here, the functional interdependency  $p^c(s^l)$  is given by a formulation according to van Genuchten (1980)

$$p^c = p^r \left[ [s^l]^{-\frac{1}{m}} - 1 \right]^{\frac{1}{n}} \quad (20)$$

with the material parameters  $p^r$ ,  $n$  and  $m$ , which are used to fit the model to the experimental data.

It turns out from general thermodynamical considerations, that the stress state of the skeleton  $\varphi^s$  and the pore fluids  $\varphi^\beta$  is separated into two parts (Ehlers 2002):

$$\boldsymbol{\sigma}^s = \boldsymbol{\sigma}^{s'} - \phi^s p \mathbf{1}, \quad \boldsymbol{\sigma}^\beta = \boldsymbol{\sigma}^{\beta'} - \phi^\beta p^\beta \mathbf{1}. \quad (21)$$

Therein, the effective stress  $\boldsymbol{\sigma}^{s'}$  results from the deformation of the skeleton  $\varphi^s$  while the frictional stress  $\boldsymbol{\sigma}^{\beta'}$  is associated with the flow of the pore fluid  $\varphi^\beta$ . The pore pressure  $p$  in equation (21) is given through Dalton's law:

$$p = s^l p^l + [1 - s^l] p^g. \quad (22)$$

The gas pressure  $p^g$  is related to the material density  $\varrho^g$  by the ideal gas law:

$$\varrho^g = \frac{\mathcal{M}^g}{RT} p^g. \quad (23)$$

In equation (23),  $\mathcal{M}^g$  denotes the molar mass of  $\varphi^g$ ,  $R$  the universal gas constant and  $T$  the temperature.

The overall stress tensor  $\boldsymbol{\sigma}$  of the porous material is given by the sum of the partial stress tensors  $\boldsymbol{\sigma}^\alpha$ . Neglecting the frictional stresses  $\boldsymbol{\sigma}^{\beta'} \approx \mathbf{0}$  in (21)<sub>2</sub> one obtains

$$\boldsymbol{\sigma} = \boldsymbol{\sigma}^{s'} - p \mathbf{1} \quad (24)$$

in analogy to the concept of effective stress (Bishop 1959).

Furthermore, it is assumed that the transport of the pore fluids  $\varphi^\beta$  is governed by DARCY's law

$$\phi^\beta \mathbf{w}_\beta = - \frac{k_r^\beta k_0}{\mu^\beta} \text{grad}(p^\beta). \quad (25)$$

Herein,  $\mu^\beta$  represents the dynamic viscosity of the pore fluid and  $k_0$  is the intrinsic permeability of the porous material. The relative permeability  $k_r^\beta$  takes into account the dependence of the overall permeability on the saturation. In conjunction with (19), van Genuchten (1980) derived the following expressions:

$$\begin{aligned} k_r^l &= \sqrt{s^l} \left[ 1 - \left[ 1 - [s^l]^{\frac{1}{m}} \right]^m \right]^2, \\ k_r^g &= \sqrt{1 - s^l} \left[ 1 - [s^l]^{\frac{1}{m}} \right]^{2m}. \end{aligned} \quad (26)$$

To close the description of the proposed model, the effective stress  $\boldsymbol{\sigma}^{s'}$  in (24) has to be specified. For the modeling of brittle failure, an isotropic damage model characterized by a single damage parameter  $d$  and a strain based description of the damage evolution is used (Simo and Ju 1987). As a means of regularization, a gradient enhanced formulation is adopted (Peerlings et al. 1996).

Physically, degradation of the material properties results from the initiation and growth of microcracks in the skeleton. For the isotropic damage case, the microcracks may be interpreted as spherically, uniformly distributed pores with the apparent volume fraction  $\phi^m$ . Based on this idea, the damaged stiffness tensor  $\mathcal{C}$  of the skeleton  $\varphi^s$  is given by

$$\mathcal{C} = [1 - \phi^0 - \phi^m] \mathcal{C}^s, \quad \mathcal{C}^s = 2\mu^s \mathcal{I} + \lambda^s \mathbf{1} \otimes \mathbf{1}, \quad (27)$$

where  $\phi^0$  is the porosity and  $\mu^s, \lambda^s$  are the Lamé constants of the skeleton material. The apparent porosity  $\phi^m$  is related to the damage parameter  $d$  according to the formula:

$$\phi^m = [1 - \phi^0]d. \quad (28)$$

Considering the expansion resulting from ASR by means of the volumetric strain  $\varepsilon_s^a$  and using equation (27), the effective stress reads:

$$\boldsymbol{\sigma}^{s'} = \mathbf{C} : [\boldsymbol{\varepsilon}_s - \varepsilon_s^a \mathbf{1}]. \quad (29)$$

As mentioned above, the ASR swelling of the skeleton results from the variation of the material density  $\rho^s$  of the skeleton, compare equation (15). Consequently, the expansion  $\varepsilon_s^a$  is defined as

$$\varepsilon_s^a = \frac{\rho_0^s}{\rho^s} - 1, \quad (30)$$

where  $\rho_0^s$  denotes the initial material density of the skeleton. Inserting the material density of the skeleton  $\rho^s$  according to equation (15) and the initial value  $\rho_0^s = \rho^u$  into equation (30) yields the ASR expansion  $\varepsilon_s^a$  as function of the reaction extent  $\xi$  for constant environmental conditions:

$$\varepsilon_s^a = \left[ \frac{\rho^u}{\rho^r} - 1 \right] \xi. \quad (31)$$

The damage parameter  $d$  is an explicit function of the internal variable  $\kappa$ , which represents the most severe deformation the material has experienced. The evolution of  $\kappa$  is governed by the criterion

$$\Phi = \bar{\eta} - \kappa \leq 0, \quad (32)$$

where  $\bar{\eta}$  denotes the non-local equivalent strain. From the Kuhn-Tucker loading/unloading conditions and the consistency condition

$$\Phi \leq 0, \quad \frac{\partial \kappa}{\partial t} \geq 0, \quad \Phi \frac{\partial \kappa}{\partial t} = 0, \quad \frac{\partial \Phi}{\partial t} \frac{\partial \kappa}{\partial t} = 0 \quad (33)$$

follows, that  $\kappa$  is unchanged for  $\Phi < 0$  and calculated by  $\kappa = \bar{\eta}$  otherwise.

The non-local equivalent strain  $\bar{\eta}$  in equation (32) is calculated on the basis of the following differential equation:

$$\eta = \bar{\eta} - \text{div}(g \text{ grad}(\bar{\eta})). \quad (34)$$

Herein,  $\eta$  denotes the equivalent strain representing a scalar measure of the local deformation state. The

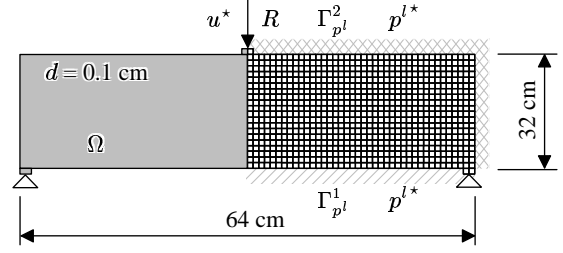


Figure 1: Geometry, mechanical and hygral boundary conditions and finite element mesh.

chosen equivalent strain  $\eta$  corresponds to the Rankine criterion of maximal principal stress:

$$\eta = \frac{\lambda^s + \mu^s}{\mu^s [3\lambda^s + 2\mu^s]} \max \langle \tilde{\sigma}_i^{s'} \rangle, \quad i = 1, 2, 3, \quad (35)$$

with  $\max \langle \tilde{\sigma}_i^{s'} \rangle$  denoting the positive part of the largest eigenvalue of the undamaged effective stress

$$\tilde{\boldsymbol{\sigma}}^{s'} = \frac{1 - \phi^0}{1 - \phi^0 - \phi^m} \boldsymbol{\sigma}^{s'} = \sum_{i=1}^3 \tilde{\sigma}_i^{s'} \mathbf{n}^i \otimes \mathbf{n}^i. \quad (36)$$

Due to the gradient parameter  $g$  in equation (34) with the dimension of length squared an internal length scale is present in the formulation.

Finally, the damage parameter  $d$  is given by

$$d = 1 - \frac{\kappa_0}{\kappa} [1 - \alpha_1 + \alpha_1 \exp(\alpha_2 [\kappa_0 - \kappa])], \quad (37)$$

where  $\alpha_1, \alpha_2$  are material parameters, which control the post-peak slope of the tensile stress-strain curve, when the initial damage threshold  $\kappa_0$  is exceeded.

### 3 NUMERICAL APPLICATION

The model proposed in the previous section is based on standard hygro-mechanical material parameters and on chemical material parameters ( $\rho^u, \rho^r, k$ ), which control the deterioration caused by ASR. The chemical material parameters are well-defined and can be easily determined by means of macroscopic strain measurements on reactive concrete specimens (Bangert et al. 2003): the parameter  $\rho^u / \rho^r - 1$  represents the asymptotic strain in a stress-free expansion test and the parameter  $k$  controls the slope of the respective expansion-time-relation at the onset of ASR. The more humid the ambient conditions, the faster (higher  $k$ ) and the more intensive (higher  $\rho^u / \rho^r - 1$ ) the alkali-silica reaction occurs.

In order to study the deterioration mechanisms of ASR on structural level, an ASR-affected concrete beam is simulated by using the hygro-chemo-mechanical model proposed in Section 2. In this

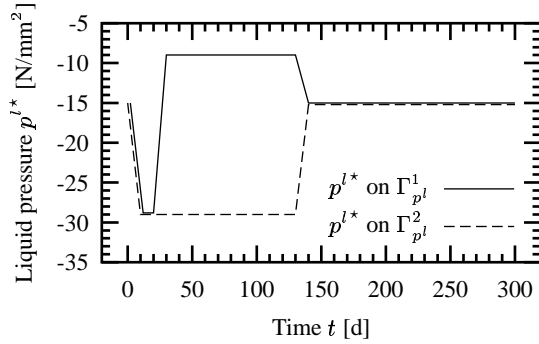


Figure 2: Hygral loading history.

numerical example, plane strain conditions are assumed. For the sake of simplicity, the gas pressure  $p^g$  is neglected ( $p^g = 0$  in  $\Omega$ ). A description of the applied numerical solution technique within the Finite Element Method and a documentation of the mechanical, chemical, hygral material parameters are given in Bangert et al. (2003).

Figure 1 contains the geometry, the mechanical support conditions, the hygral Dirichlet boundaries  $\Gamma_{p^l}^1$  and  $\Gamma_{p^l}^2$ , and the spatial discretization with finite elements. To avoid stress oscillations in connection with the gradient enhanced damage formulation, the displacements  $\mathbf{u}_s$  and the liquid pressure  $p^l$  are interpolated with quadratic shape functions while linear interpolations are used for the non-local equivalent strain  $\bar{\eta}$  (Peerlings et al. 1996).

The diagram in Figure 2 illustrates the hygral loading history. The initial conditions are given by  $\mathbf{u}_{s0} = \mathbf{0}$  for the displacements and  $p_0^l = -15 \text{ N/mm}^2$  for the liquid pressure corresponding to an initial liquid saturation of  $s_0^l = 0.8$ . In an initial phase (Phase I), drying is simulated by decreasing the liquid pressure from the initial value  $p^{l*} = p_0^l$  to  $p^{l*} = -29 \text{ N/mm}^2$  corresponding to a liquid saturation of  $s^{l*} = 0.6$ . After 20 days of drying, the liquid pressure  $p^{l*}$  at the bottom of the beam is raised to  $p^{l*} = -9 \text{ N/mm}^2$  corresponding to a liquid saturation of  $s^{l*} = 0.9$  (Phase II). Thus, a moisture transport oriented from the bottom to the top is imposed. In the third loading phase starting at  $t = 130 \text{ d}$ , all hygral boundary conditions are reset to the initial value  $p^{l*} = p_0^l$  and held constant afterwards.

Concerning the non-local equivalent strain  $\bar{\eta}$ , the natural boundary condition  $\text{grad}(\bar{\eta}) \cdot \mathbf{n} = 0$  is adopted (Peerlings et al. 1996).

### 3.1 Deterioration mechanisms

Figure 3 illustrates, from the left to the right, the distribution of the liquid saturation  $s^l$ , the ASR expansion rate  $\partial \varepsilon_s^a / \partial t$ , the ASR expansion  $\varepsilon_s^a$  and the damage parameter  $d$  at selected stages of the hygral loading history. The first row of Figure 3 ( $t = 20 \text{ d}$ ) corresponds to the end of the initial drying process. Due to drying of the surface, the alkali-silica reaction takes place with a much greater intensity in the more humid inner part characterized by larger values of the ASR expansion  $\varepsilon_s^a$  and the respective expansion rate  $\partial \varepsilon_s^a / \partial t$ . Since the ASR-induced expansion of the core is at least partially hindered, the inner part of the beam is subjected to compression while the outer part is subjected to tension. These tensile stresses cause cracking along the surface. The opening of such surface cracks is frequently observed in ASR-affected concrete structures.

The contour plots in Figure 3 for  $t = 40 \text{ d}$  to  $t = 120 \text{ d}$  correspond to the wetting process (Phase II) characterized by a moisture transport oriented from the bottom towards the top. Accordingly, the ASR-induced expansion accelerates at the bottom face of the beam as is reflected for  $t = 40 \text{ d}$  by high values of the expansion rate  $\partial \varepsilon_s^a / \partial t$ . At this stage, the ASR expansion  $\varepsilon_s^a$  within the inner part of the beam is still larger compared to the expansion within the outer parts of the beam. However, the simultaneous moisture diffusion into the beam and the activation of reaction kinetics within the more humid zone near the surface leads to the formation of an ASR front which starts to propagate from the bottom to the top (from  $t = 60 \text{ d}$  to  $t = 120 \text{ d}$ ). In front of the highly affected lower part of the beam, i.e. in the region characterized by a large spatial gradient of the expansion  $\varepsilon_s^a$ , the concrete is subjected to tensile stresses, which exhaust the tensile strength and lead to substantial cracking in the vicinity of the ASR front.

The last two rows in Figure 3 correspond to hygral unloading (Phase III), i.e. the liquid pore pressure at all surfaces is reset to the initial value ( $p^{l*} = p_0^l$ ) and held constant afterwards. From time  $t = 140 \text{ d}$  to the end of the numerical simulation ( $t = 300 \text{ d}$ ), only marginal changes of the damage state are observed. This reflects the fact, that the alkali-silica reaction has almost completely come to an end ( $\partial \varepsilon_s^a / \partial t \approx 0$ ). It should be noted, that in a purely hygro-mechanical analysis (i.e.  $\varepsilon_s^a = 0$ ) corresponding to a beam made of concrete containing no reactive silica within the aggregates, no damage

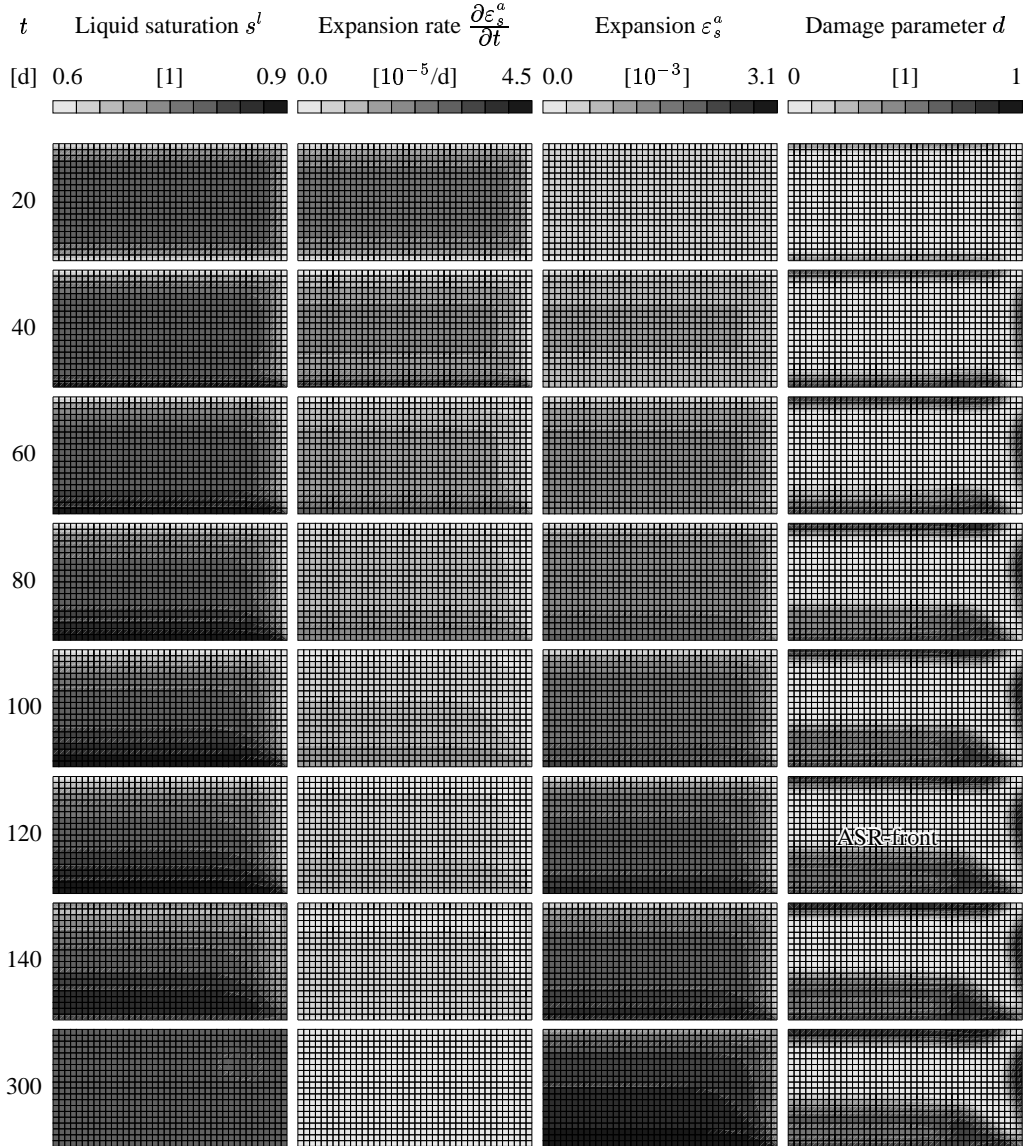


Figure 3: Distribution of the liquid saturation  $s^l$ , the expansion rate  $\partial \varepsilon_s^a / \partial t$ , the expansion  $\varepsilon_s^a$  and the damage parameter  $d$  at different stages of the loading history.

would be observed (i.e.  $d = 0$ ) for the hygral loading scenario considered in this analysis.

### 3.2 Structural degradation

The structural degradation, i.e. the reduction of the ultimate load and of the structural stiffness resulting from the ASR expansion, is investigated. To this end, three point bending tests are performed numerically by applying a displacement driven load  $R$  in the center of the beam at two stages of the loading history. The application of the displacement  $u^*$  is

controlled by the load factor  $\lambda$ .

The diagram in Figure 4 contains the load-displacement relations  $R(\lambda)$  from both ultimate load analyses. Obviously, the structural stiffness  $E$  and the ultimate load  $R^u$  are significantly reduced during 300 days of ASR expansion. Furthermore, at time  $t = 300$  d a more brittle structural response is observed in the very early post-peak regime compared to  $t = 0$  d. The structural stiffness is reduced by  $[1 - E_{300}/E_0] = 55\%$  due to the alkali-silica reaction whereas the ultimate load is

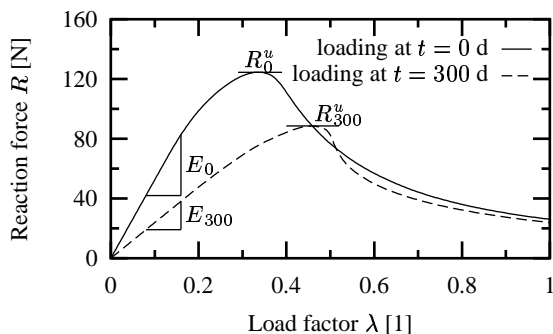


Figure 4: Load-displacement diagrams  $R(\lambda)$  of the virgin concrete beam (ultimate load analysis at  $t = 0$  d) and the ASR-affected concrete beam (ultimate load analysis at  $t = 300$  d).

decreased by  $[1 - R_{300}^u/R_0^u] = 27\%$ . These values underline the severe consequences of concrete deterioration caused by ASR on the structural safety.

#### 4 CONCLUSIONS

In this paper, a macroscopic model for ASR-affected concrete was developed within the framework of the Theory of Porous Materials. The alkali-silica reaction is regarded as a two-stage process: non-instantaneous gel formation + instantaneous swelling of gel. In the proposed model the dependence of the kinetics and the magnitude of the swelling process on the moisture content is taken into account.

On the structural level numerical simulations of a concrete beam affected by the alkali-silica reaction has illustrated, that the moisture dependence of the alkali-silica reaction can explain the detrimental impact of ASR on the stiffness, strength and stability of concrete structures. Even a slightly non-uniform distribution of the moisture content leads to the formation of an ASR front propagating through the structure. Thereby, less humid parts are subjected to tensile stresses which are balanced by compressive stresses within the more humid regions. If the tensile stresses exceed the tensile strength, diffusive cracking is induced resulting in a mode of deterioration typically observed in ASR-affected concrete structures.

#### 5 ACKNOWLEDGMENT

Financial support was provided by the German National Science Foundation (DFG) in the framework of project A9 of the collaborative research center SFB 398. This support is gratefully acknowledged.

#### REFERENCES

- Atkins, P. (1998). *Physical chemistry*. Oxford: Oxford University Press.
- Bangert, F., D. Kuhl, and G. Meschke (2003). Chemo-hydro-mechanical modeling and numerical simulation of concrete deterioration caused by alkali-silica reaction. *International Journal for Numerical and Analytical Methods in Geomechanics*. submitted.
- Bishop, A. (1959). The concept of effective stress. *Teknisk Ukeblad* 39, 859–863.
- Dent Glasser, L. and N. Kataoka (1981). The chemistry of alkali-aggregate reaction. *Cement and Concrete Research* 11, 1–9.
- Dron, R. and F. Brivot (1993). Thermodynamic and kinetic approach to the alkali-silica reaction. Part 2: Experiment. *Cement and Concrete Research* 23, 93–103.
- Ehlers, W. (2002). Foundations of multiphase and porous materials. In W. Ehlers and J. Bluhm (Eds.), *Porous media – Theory, experiments and numerical applications*, pp. 3–86. Berlin: Springer.
- Glasser, F. (1992). Chemistry of the alkali-aggregate reaction. In R. Swamy (Ed.), *The alkali-silica reaction in concrete*, Chapter 2, pp. 30–53. Glasgow, London: Blackie and Son Ltd.
- Larive, C. (1998). *Apports combinés de l'expérimentation et de la modélisation à la compréhension de l'alcali-réaction et de ses effets mécaniques*. Ph. D. thesis, Laboratoire Central des Ponts et Chaussées, Paris.
- Peerlings, R., R. de Borst, W. Brekelmans, and J. de Vree (1996). Gradient enhanced damage for quasi-brittle materials. *International Journal for Numerical Methods in Engineering* 39, 3391–3403.
- Simo, J. and J. Ju (1987). Strain and stress-based continuum damage models I - Formulation. *International Journal for Solids and Structures* 23, 821–840.
- Steffens, A., K. Li, and O. Coussy (2003). Aging approach to water effect on alkali-silica reaction degradation of structures. *Journal of Engineering Mechanics (ASCE)* 129(1).
- Struble, L. and S. Diamond (1981). Unstable swelling behaviour of alkali silica gels. *Cement and Concrete Research* 64, 611–617.
- Ulm, F.-J., O. Coussy, L. Kefei, and C. Larive (2000). Thermo-chemo-mechanics of ASR expansion in concrete structures. *Journal of Engineering Mechanics (ASCE)* 126, 233–242.
- van Genuchten, M. (1980). A closed-form equation for predicting the hydraulic conductivity of unsaturated soils. *Soil Science Society of America* 44, 892–898.